old Sections 3.7 and 3.8 PhL 5.11.14

3.7 The general shape of fields, charges, and currents on a transmission line

(a) Facts about field structure

Based on the information in Table 2 (3.6.1) above, we are in a position to draw the general field structure for a real transmission line. Some general rules are now apparent:

Fact 1: In a *cross sectional* sketch of a transmission line, the **E** field lines land on the conductors at right angles to the conductor surface. This is exactly true for the TEM mode, and applies to all points on the conductor surfaces. (3.7.1)

Proof: There are no transverse surface currents in the TEM mode, so $E_\theta = 0$ exactly. Even if this were not true, we would expect the right angle rule to be very nearly exact, since transverse E fields must in any event be miniscule. See Fact 2 following as well as the discussion of Appendix D.8.

Fact 2: In a *longitudinal* sketch of a transmission line, the E fields still land on the conductors at very close to right angles. (3.7.2)

Proof: The deviation from $\pi/2$ is less than 10^{-4} radians according to (3.6.2), and the deviation is in the direction of current flow at each conductor. This causes a very slightly warping of the otherwise planar cross-sectional field line grid.

Fact 3: Apart from an overall scale factor, the cross-sectional field shape of a TEM wave on a transmission line is independent of position z along the transmission line, and is independent of time t. The shape is also independent of ω. (3.7.3)

Proof: As we shall see below, the TEM form of any field or current is $\mathbf{F}(x,y,z,t) = e^{j[\omega t - kz + \varphi_F(\omega)]}\mathbf{F}(x,y)$ where **F**(x,y) is real, so all t and z dependence is in the exponential. We can take the physical field to be the real part as discussed in Section 1.6 so $\mathbf{F}_{physical}(x,y,z,t) = \cos[\omega t - kz + \varphi_F(\omega)]\ \mathbf{F}(x,y)$. Thus, the cross sectional shape of the field is determined by **F**(x,y) and is the same at all values of z apart from an overall scale factor $\cos[\omega t - kz + \varphi_F(\omega)]$. This scale factor varies between +1 and -1 as one moves down the line in z at some fixed t, or as one observes at some fixed z as time varies. Later we will see that this shape **F**(x,y) can be found by solving a certain 2D Helmholtz equation, and we find that the shape is determined entirely by the shape of the boundaries of the conductors. Different vector fields (e.g., **J** and **E**) might have different phases in this wave motion which we indicate by $\varphi_F(\omega)$ for **F**(x,y,z,t).

Fact 4: In a cross sectional sketch of a transmission line operating at high frequency, the **E** and **B** field lines are perpendicular at every point in the dielectric. (3.7.4)

Proof: From Maxwell's curl E equation (1.1.2) in the ω domain we have

$$\text{curl}\ \mathbf{E} = -j\omega\mathbf{B}\ . \qquad (1.1.2)$$

Then

$$\mathbf{B} \bullet \mathbf{E} = (-j\omega)^{-1} \, \mathbf{curl\ E} \bullet \mathbf{E}$$

$$= (-j\omega)^{-1} \left[\left(\partial_x E_y - \partial_y E_x \right) E_z + \left(\partial_y E_z - \partial_z E_y \right) E_x + \left(\partial_z E_x - \partial_x E_z \right) E_y \right] . \qquad (3.7.5)$$

To the extent that $E_z << E_x$ and E_y, we set $E_z \approx 0$ (and $\partial_y E_z$ and $\partial_x E_z$) to get

$$\mathbf{B} \bullet \mathbf{E} = (-j\omega)^{-1} \left[- \left(\partial_z E_y \right) E_x + \left(\partial_z E_x \right) E_y \right] + (-j\omega)^{-1} \left[\text{correction terms} \right]$$

where "correction terms" accounts for the fact that the dismissed terms are not exactly zero. Then

$$\mathbf{B} \bullet \mathbf{E} = (-j\omega)^{-1} \left[E_y^2 \, \partial_z (E_x / E_y) \right] + (-j\omega)^{-1} \left[\text{correction terms} \right] . \qquad (3.7.6)$$

However, we argued in Fact 3 that the shape of fields does not vary with z. Thus, the ratio of two components like E_x/E_y cannot vary with z. Thus $\partial_z (E_x/E_y) = 0$ so

$$\mathbf{B} \bullet \mathbf{E} = (-j\omega)^{-1} \left[\text{correction terms} \right] .$$

Letting α be the angle between **B** and **E**, we can write

$$|\mathbf{B}| \, |\mathbf{E}| \cos\alpha = (\omega)^{-1} \, | \text{correction terms} |$$

so then

$$\cos\alpha = (\omega)^{-1} \, | \text{correction terms} | \, / \, (|\mathbf{B}| \, |\mathbf{E}|) . \qquad (3.7.7)$$

Since the correction terms involve E_z which is very small, the correction terms are presumably small compared to $(|\mathbf{B}| \, |\mathbf{E}|)$ and we then conclude that $\cos\alpha \approx 0$ and $\alpha \approx \pi/2$ and then $\mathbf{B} \bullet \mathbf{E} = 0$.

However, for sufficiently small ω the right side of (3.7.7) blows up and our conclusion is no longer valid. A condition for validity would then be

$$\cos\alpha << 1$$

or

$$(\omega)^{-1} \, | \text{correction terms} | \, / \, (|\mathbf{B}| \, |\mathbf{E}|) << 1$$

or

$$\omega >> | \text{correction terms} | \, / \, (|\mathbf{B}| \, |\mathbf{E}|)$$

In particular, this condition is violated when $\omega \approx 0$.

Example: In Figure C.2 we can imagine the rectangular conductor shown to be the center conductor of a very large radius coaxial transmission line operating at very low frequency. Fact 1 tells us that **E** is normal to the conductor surface, but clearly **H** is not normal, so $\mathbf{E} \bullet \mathbf{B} \neq 0$.

Reader Exercise: Find a ballpark expression for ω_1 such that $\omega >> \omega_1$ gives $\cos\alpha \approx 0$ so $\mathbf{B} \bullet \mathbf{E} = 0$. Perhaps calculate a value for ω_1 for the transmission line considered in Chapter 6.

Fact 5: In a cross sectional sketch of a transmission line operating above very low frequencies, the **B** field lines just outside the conductor surfaces are parallel to the surface, so $\mathbf{B} = B_\theta \hat{\boldsymbol{\theta}}$ in Fig 3.3. Thus, $B_r = 0$ at the surface. (3.7.8)

Proof: We have shown in Fact 4 that above very low frequencies, the **B** lines must be perpendicular to the **E** lines everywhere in the dielectric, and this includes just outside the conductor. But from Fact 1 we know that $\mathbf{E} = E_r \hat{\mathbf{r}}$ at the surface. Therefore $B = B_\theta$ and $B_r = 0$. This then is the justification for maintaining the condition $B_r = 0$ in Table 2 where we have a non-perfect conductor.

Comment: Fact 5 is a non-trivial and non-obvious fact, and applies to arbitrarily shaped conductor cross sections, as do all our facts here. The result seems obvious for round wires, but is in fact non-obvious even in that case. If a transmission line is made of two fat round conductors closely spaced, one imagines that the B lines due to current in one conductor are perfectly circular about the center of that conductor. In fact this must be false, because we are claiming in Fact 5 that the vector sum of *both* conductor's B fields (ie, the total or actual B field) has a round contour line at the surface of each conductor. Thus, the B field contours due to one conductor alone must not be circular. In fact, the current density inside each conductor is non-uniform by just the right amount to make this work out. For widely spaced round conductors, the effect is not very noticeable because the effect of one conductor's B field at the surface of the other conductor is so small.

(b) Drawings of the fields

We are now in a position to draw some sketches of fields on a transmission line. Let's start with the transverse or cross section picture:

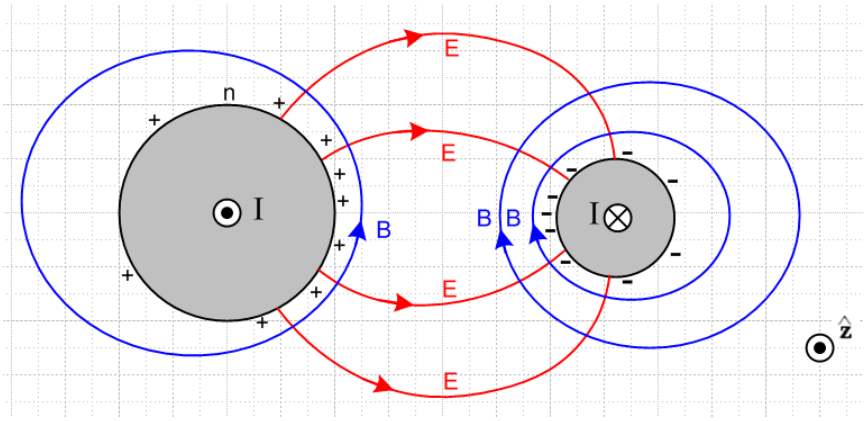

Fig 3.5

Fig 3.5: Cross section view

Although this figure is drawn for two round conductors, its general features apply to any conductors. The figure is a snapshot at one instant in time. The • and ⊗ indicate current flow direction in the conductors. Positive charge exists on the surface of the left conductor, and is strongest on the face of that conductor which is closest to the other conductor. Negative surface charge lies on the right conductor. The electric

fields are as shown and are strongest in the region between the conductors. The magnetic field directions derive from the right hand rule relative to the current in each conductor. The lines of E and B always intersect at right angles as noted in (3.7.4).

The magnitude of the E field is determined by the potential difference between the conductors and the geometry. It is independent of frequency. Similarly, the magnitude of the B field is determined by the size of the current in either conductor and is also independent of frequency.

Consider a 75 Ω transmission line that is properly terminated and is driven by a 7.5 volt amplitude sine wave. Regardless of frequency ω, the magnitude of the current in this transmission line is 100 mA, and the magnitude of the potential difference is 7.5 volts. Of course both these quantities have sinusoidal time dependence. At some instant in time, the fields and currents are as in Fig 3.5.

We have just argued then that not much happens in the transverse directions x and y as frequency sweeps from very low to very high. Of course the rate at which the pattern oscillates back and forth increases, but the shape of things does not change. At the peak of each cycle, things look like Fig 3.5 regardless of ω.

This may seem contradictory. In general, one is used to ω affecting things due to equations like

curl **E** = -jω**B** Maxwell curl E equation *(1.1.2)*

The resolution is that all the spatial variation happens in the *longitudinal* direction. Here then is a top view of the same transmission line:

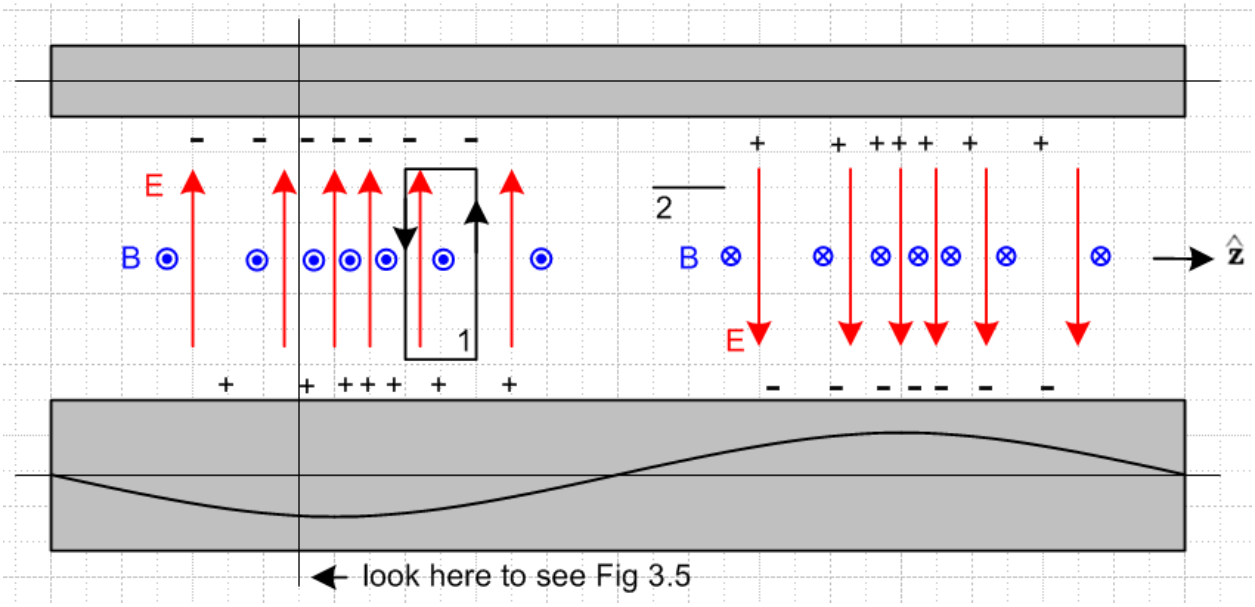

Fig 3.6: Top view of transmission line Fig 3.6

The red E arrows are all of unit length and serve to mark the direction and density of electric field lines lying in the plane containing the center lines of the conductors. The blue B arrows are seen end-on and indicate the same for the magnetic field. On the left they come out of the plane of paper and on the right they go into it. Later we shall learn about the "transmission line limit" in which the wavelength λ of the wave propagating down a transmission line is assumed to be much larger than all transverse dimensions of the line. The reader should understand the above picture as being in that limit, but one would have to

stretch the picture at least 10X horizontally to make it be reasonable. At all places **E**x**B** points to the right, so we have a wave propagating to the right (+z).

Now apply the Maxwell curl equations using the two loops shown. Loop 1 is positioned to pick up magnetic flux, so we use (1.1.36) which in the frequency domain says

$$\text{curl } \mathbf{E} = -j\omega\mathbf{B} \qquad \Leftrightarrow \qquad \oint \mathbf{E} \bullet d\mathbf{s} = -j\omega[\int_S \mathbf{B} \bullet d\mathbf{S}] \tag{3.7.9}$$

Notice the ω sitting on the right side. We argued in the last section that the amplitude of the B field does not change as ω changes. Thus, the right side of (3.7.2) is proportional to ω. As ω increases, the line integral of the E field around loop 1 must increase. Thus, the rate of change of E must increase in the z direction! In other words, as ω increases, the whole pattern of Fig 2 contracts in the z direction, which causes all z derivatives to increase, thus increasing $\oint \mathbf{E} \bullet d\mathbf{s}$ for the same fixed loop 1. Remember that the strength of the E field is indicated in Fig 2 by the density of the red arrows, not by the length of the red arrows.

A similar argument applies to loop 2. This loop appears end-on in Fig 2. It is set up to sense the electric field flux. The appropriate curl equation is (1.1.38) which says

$$\text{curl } \mathbf{B} = \mu\varepsilon j\omega\mathbf{E} + \mu\mathbf{J_c} \qquad \Leftrightarrow \qquad \oint \mathbf{B} \bullet d\mathbf{s} = \mu \int_S [\varepsilon j\omega\mathbf{E} + \mathbf{J_c}] \bullet d\mathbf{A}$$

$$\approx j\omega\mu\varepsilon \int \mathbf{E} \bullet d\mathbf{A} \,. \tag{3.7.10}$$

Since we are now in the dielectric, we have ignored the small leakage conduction current, and have kept the dominant displacement current. Again there is a factor of ω on the right side, arising from a time derivative. As ω increases, the line integral of the B field must increase. Thus, the B field must change faster in the z direction. As ω increases, the curl equation (3.7.2) is satisfied by having the entire pattern contract in the z dimension.

If the frequency ω doubles, the wavelength λ goes to half. This of course is no surprise, since ω and λ are related by the speed of light v in the dielectric,

$$\lambda = v/f = 2\pi v/\omega \,. \tag{3.7.11}$$

The main point of the above discussion is to show how the Maxwell curl equations force the field pattern to contract in the z direction as ω increases. In the transverse direction, the field pattern *shape* stays constant.

(c) More on the field and current structure

Here we explore in more detail the general distribution of fields and currents in a transmission line. The goal is to establish the phase relationships among the electromagnetic fields and various currents. Once this is done, it is possible to make an estimate of the ratio J_r/J_z and that is done in the following section.

Consider the following more elaborate version of Figure 3.6 :

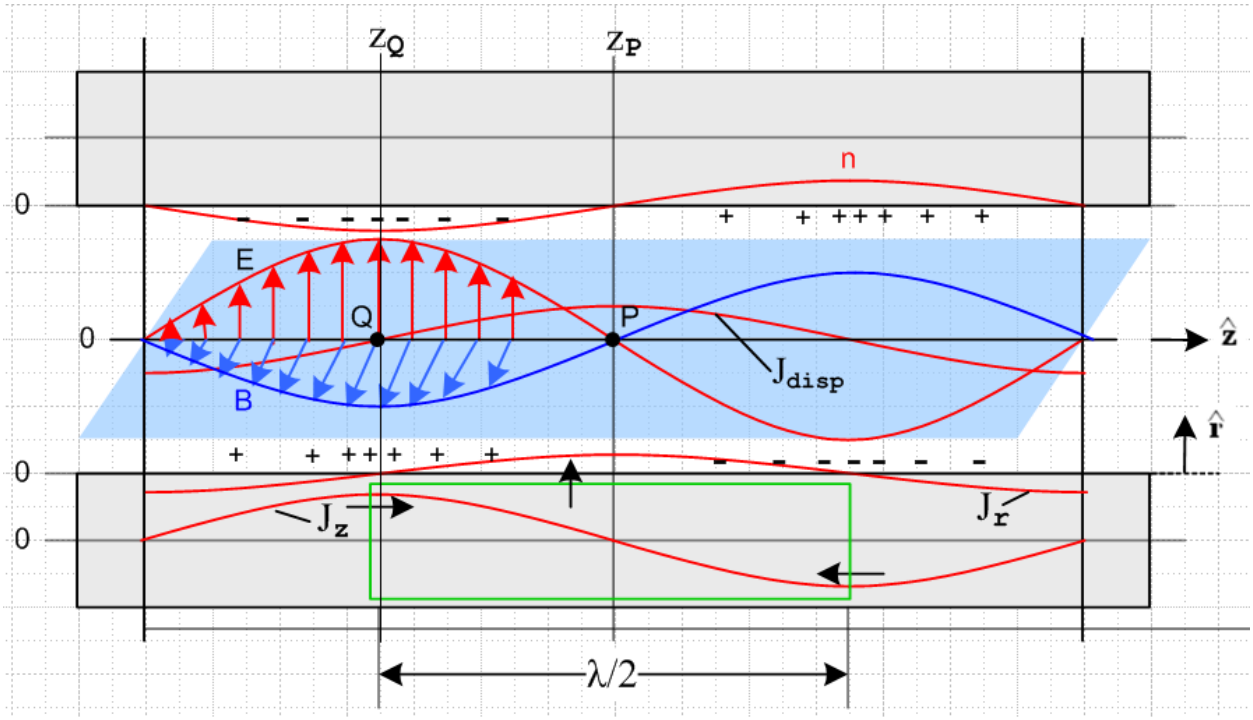

Tilted overhead view of a transmission line Fig 3.7

The picture is quite complicated and deserves clarifying comments:

(1) Unlike in Fig 3.6, the E and B arrows indicate the **E** and **B** vectors, and are not just field direction and field line density indicators.

(2) The **E** and **B** field vectors are shown along some line which lies in the plane of the center lines of the two conductors and which points in the $\hat{\mathbf{z}}$ direction, as do those center lines.

(3) The blue **B** field arrows lie in the blue plane which is meant to be perpendicular to the plane of the conductor center lines, which is the plane of paper. The red **E** field arrows are in the plane of paper.

(4) Looking at **E** x **B**, we see that the wave is traveling to the right in the $\hat{\mathbf{z}}$ direction.

(5) The **E** field arrows point from positive charge to negative charge, so this is why the + and - signs are distributed as shown.

(6) The conductors are fixed to the paper, everything else is moving to the right at velocity v. This includes the **E** and **B** arrows and their curves, the charge density and its curve n, and the two current curves drawn on the bottom conductor.

(7) At point Q on plane $z = z_Q$, since **B** is coming out of paper to the viewer, the longitudinal current J_z in the lower conductor must be pointing to the right. This is why J_z is shown positive at this point in the lower conductor, and this calibrates the position of the J_z curve. Maximum J_z occurs with maximum B.

(8) There exists a displacement current $\mathbf{J_{disp}} = \partial_t \mathbf{D} = \varepsilon \partial_t \mathbf{E}$ in the dielectric whose magnitude is shown as a red curve. For an observer sitting at fixed point P, since the wave is moving to the right, the value of $\partial_t \mathbf{E}$ is at its instantaneous maximum positive value. This is why the red J_{disp} curve has a positive maximum at point P.

(9) As discussed in Section 3.4, the displacement current is "fed" by the radial current J_r inside the lower conductor, so the J_r curve also has its maximum positive value at point P. This J_r current is busily radially pumping positive charge to the surface of the lower conductor at point P so that charge will be there when the wave has moved λ/4 to the right. Of course this radial J_r is doing this charge pumping all around the lower conductor, but we only show it in the plane of paper.

(10) We have glossed over the fact that the E and B fields track each other in magnitude. For example, they are both maximal at the same longitudinal position z_Q. B is maximum there because J_z is maximum, but it is not quite clear why E is maximal at the same point. We know this alignment occurs in a plane wave, but a transmission line TEM mode is not *just* a plane wave. Various arguments can be ginned up for the alignment of the E and B maximums. One simple argument involves the green cylindrical Gaussian box drawn inside the lower conductor, and we reverse the discussion above. Note that this box lies entirely inside the conductor and so does not enclose any surface charge. Since there can be no charge inside a conductor, this box has $Q_{enclosed} = 0$. Thus, the total current flowing into this box must be zero. Since the J_z current flows into both ends of this box (black arrows), the J_r current has to flow out on the cylinder's curved surface. By considering shorter green boxes one can show that J_r is maximal at z_P (as drawn). Thus J_{disp} is maximum at z_P which means $\partial_t E$ must be maximum there, which means E = 0 at z_P which means E has its maximum in alignment with the maximum of B.

(d) Estimate of the ratio J_r/J_z

Having drawn and described this elaborate picture, we now consider again the green Gaussian box. At the instant in time for which Fig 3.7 is drawn, the total current flowing into the endcaps of the box is 2I, where I is the peak longitudinal current -- the magnitude of the longitudinal sine wave. Therefore, the total J_r integrated over the sides of the green cylinder must also be 2I.

To obtain a ballpark estimate of the situation, we first assume that the two round conductors are far apart compared to their radii, in which case J_r is roughly symmetric around the conductor surface. Then the total radial current emitted by the curved surface of the green Gaussian cylinder is:

$$\text{radial current total} = [\,(2/\pi)J_r\,] * 2\pi a * (\lambda/2) = 2I$$

Since J_r is a longitudinal sine wave, we have added a factor $2/\pi$ to get its value averaged over the length of the Gaussian box. In a more general case, we can replace $2\pi a$ with distance p which represents the active portion of the conductor perimeter, as illustrated in Fig 2.14. Then we have

$$[\,(2/\pi)J_r\,] * p * (\lambda/2) = 2I \quad \Rightarrow$$

$$J_r = 2\pi I / (\lambda p) \quad . \qquad (3.7.12)$$

On the other hand, for a round conductor operating in the skin effect regime where $\delta < a$,

$$J_z \approx I/(p\delta) \tag{3.7.13}$$

where p is the same active perimeter just mentioned. So

$$J_r/J_z \approx 2\pi\,(\delta/\lambda)\ . \tag{3.7.14}$$

For δ we had

$$\delta \equiv \sqrt{2/\omega\mu\sigma}\ . \tag{2.2.20}$$

From (3.7.11) we have $\lambda = v/f = 2\pi v/\omega$ where v is the wave phase velocity. Then

$$(\delta/\lambda) = \sqrt{\frac{2}{\omega\mu\sigma}}\ \frac{\omega}{2\pi v} = \sqrt{\frac{2\omega}{\mu\sigma}}\ \frac{1}{2\pi v} = \sqrt{\frac{4\pi f}{\mu\sigma}}\ \frac{1}{2\pi v}\ . \tag{3.7.15}$$

Setting $v \approx c$ and $\mu = \mu_0 = 4\pi \times 10^{-7}$ and $\sigma = 5.81 \times 10^{7}$ (copper) and $f = 10^{9} f(\text{Ghz})$ we get

$$(\delta/\lambda) \approx \sqrt{\frac{4\pi f}{\mu\sigma}}\ \frac{1}{2\pi v} = \sqrt{\frac{4\pi\, 10^{9}\, f(\text{GHz})}{4\pi \times 10^{-7} \times 5.81 \times 10^{7}}}\ \frac{1}{2\pi}\ \frac{1}{3 \times 10^{8}}$$

$$= \sqrt{\frac{10^{10}\, f(\text{GHz})}{58.1}}\ \frac{1}{2\pi}\ \frac{1}{3 \times 10^{8}} = \sqrt{\frac{f(\text{GHz})}{58.1}}\ \frac{1}{6\pi}\ 10^{-3} = 7 \times 10^{-6}\ \sqrt{f(\text{GHz})}$$

and so

$$J_r/J_z \approx (2\pi)\,(\delta/\lambda) \approx 4.4 \times 10^{-5}\ \sqrt{f(\text{GHz})}\ . \tag{3.7.16}$$

For $f \leq 10$ GHz we then find

$$J_r/J_z \leq 1.4 \times 10^{-4}\,. \qquad f \leq 10 \text{ GHz} \qquad \text{skin-effect regime} \tag{3.7.17}$$

showing that the radial charge-pumping current density J_r is much smaller than the longitudinal current density J_z in the conductor sheath.

What about the low-frequency situation with no skin-effect sheath? For simplicity, we assume now two round conductors of radius a which are widely spaced. No skin effect means roughly $\delta > a$ which means

$$\sqrt{2/\omega\mu\sigma} > a \qquad \Rightarrow \qquad \omega < 2/(\mu\sigma a^2) \qquad \text{or} \qquad \omega a/2 < 1/(\mu\sigma a)\ . \tag{3.7.18}$$

In this low frequency regime we must replace (3.7.13) by

$$J_z \approx I/(\pi a^2)\ . \tag{3.7.19}$$

Since (3.7.12) is still valid, we find now that

$$J_z \approx I/(\pi a^2)$$
$$J_r \approx 2\pi I/(p\lambda) \approx 2\pi I/(2\pi a\lambda) \approx I/(a\lambda)$$

so

$$J_r/J_z \approx \pi(a/\lambda) \approx (\pi a)(\omega/2\pi v) \approx \omega a/2v = (\omega a/2)(1/v) \quad . \tag{3.7.20}$$

Using (3.7.18) for $\omega a/2$ we get

$$J_r/J_z < 1/(\mu\sigma a v) \; . \tag{3.7.21}$$

With $\mu = \mu_0 = 4\pi \times 10^{-7}$, $\sigma = 5.81 \times 10^7$ (copper) and $v = c = 3 \times 10^8$ we find for a wire of radius 1 mm,

$$J_r/J_z < \frac{1}{4\pi * 5.81 * 10^{-3} * 3 * 10^8} = \frac{10^{-5}}{4\pi * 5.81 * 3} = 4.6 \times 10^{-8}. \quad \text{low frequency} \tag{3.7.22}$$

The conclusion is that in general $J_r << J_z$ under 10 GHz and finally we justify entries made in the tables of Sections 3.5 and 3.6. The basic fact is that the green cylinder is long, so the surface area through which J_r flows is much larger than the area through which J_z flows.

3.8 Transmission Line Preliminaries

A transmission line normally has two conductors. The cross sectional shape of these conductors is assumed constant in the direction z along the transmission line. The transverse directions are x and y.

A wave propagates down a transmission line in what is called the TEM mode. TEM means that the electric and magnetic fields of a wave traveling down the guide are transverse, as in Figures 3.5-7. What this really means is that an electromagnetic wave goes straight down the conductors as guides with no surface reflections, unlike what happens in a waveguide, see Appendix F. Apart from a small drag on the wave due to losses in the conductors, the wave proceeds with wavenumber β and velocity v as it would in an open medium. The conductors shape the **E** and **B** fields, so the wave is not a "plane wave". Nevertheless, at each point in the dielectric, **E** and **B** are perpendicular and **E x B** points down the transmission line.

We now summarize a set of basic facts about this TEM mode:

Fact 1: The major current for the TEM mode is the *longitudinal* current J_z. We just showed in the last section that $J_r << J_z$. There are no azimuthal tangential currents J_θ. (3.8.1)

Fact 2: There is no cutoff frequency one has to operate above. The TEM mode works all the way down to DC (although at low frequencies, the attenuation per wavelength may become large). See Appendix F for why this is not true in a waveguide. (3.8.2)

Corollary 2: If one operates a transmission line below the cutoff of the lowest waveguide mode, the TEM mode is the only possible way of moving energy down the line. (3.8.3)

Fact 3: The simplest expression of the boundary conditions are in terms of *potentials*, not fields, so the potential wave equations are used to solve problems. For example, a boundary condition might be that the electric potential between the two conductors is 7.5 volts at the driving end. (3.8.4)

Fact 4: The transverse components of the vector potential **A** can be neglected, so A_z is the only component of **A** we have to worry about. (3.8.5)

Proof: Consider equation (1.5.9) where both conductors have the same μ,

$$\mathbf{A}(\mathbf{x},\omega) = \frac{\mu}{4\pi}\int \mathbf{J}(\mathbf{x}',\omega)\frac{e^{-j\beta R}}{R}\,dV' \qquad (3.8.6)$$

Here, **J** represents the currents in the conductors and the volume integration is over both conductors in x,y and z, and R = |**x**-**x**'|. There is clearly going to be a strong A_z component since the predominant conductor currents are in the longitudinal direction. According to Fact 1 above, transverse currents are very small, so the corresponding transverse components of **A** will also be very small and we shall completely neglect them.

When we compute **A** in the above integral, we can still decompose **A** into A_z, A_r and A_θ . These components are, however, with respect to some fixed coordinate system located perhaps on some approximate center line between the two conductors. Thus, each potential of the pair A_r and A_θ will feel the effect of both J_r and J_θ , but these are both very small. Moreover, there is considerable cancellation which takes place as pieces of J_r and J_θ are added up in the integration. We rely mainly on the fact that J_r and J_θ are very small to conclude that A_r and A_θ may be safely neglected.

This is very different from what happens with A_z. In the region of one conductor, the summation is additive for all nearby pieces of current J_z in that conductor, assuming that the wavelength λ of longitudinal propagation is much larger than any transverse dimension. The only place A_z is small is on a longitudinal line between the conductors where their contributions cancel.

We conclude then that A_r and A_θ can be neglected relative to A_z.

Fact 5: The potential φ(x) can be identified with the transverse "voltmeter voltage" . (3.8.7)

Proof: This is not immediately obvious. The thing one measures as "voltmeter voltage" is the line integral of the electric field between two points. If **E** = - ∇φ, one can identify φ with this voltmeter voltage, but according to Eq. (1.3.1), we have an extra term to worry about,

$$\mathbf{E} = -\nabla\varphi - \partial\mathbf{A}/\partial t\ . \qquad (3.8.8)$$

However, according to Fact 4 of (3.8.5), the transverse components of **A** are negligible, so

$$\mathbf{E}_t = -\nabla_t\varphi \qquad \text{where} \quad \nabla_t \equiv \hat{\mathbf{x}}\,\partial/\partial x + \hat{\mathbf{y}}\,\partial/\partial y\ . \qquad (3.8.9)$$

If one line-integrates E_t from one conductor to the other (keeping z fixed), one gets $\varphi_1 - \varphi_2$ which is a voltage that a voltmeter would measure.

Fact 6: The potential φ is *constant* over the surface of either conductor at a fixed z. (3.8.10)

Proof: This follows from the Section 3.6 Table 3 assumption that $E_\theta = 0$. Since there is no azimuthal component of electric field at the surface, we get zero doing a line integral of **E** between any two points on the surface of a conductor in a cross section slice. According to Fact 5, this gives not only the voltmeter voltage between the start and end of such an integration, but it also gives the potential difference Δφ between these two points. Since the integration must give 0, we conclude that Δφ = 0 between any two points, so φ must be constant over the surface at fixed z.

But how do we know that $E_\theta = 0$ on a conductor surface? This somewhat delicate issue is discussed in sections (a) and (b) of Section D.8 in the context of a round wire. We shall assume it is true, even though this may depend on details of how the transmission line is "driven" at its source, and even though it might only be approximately true in that E_θ is extremely small and little error is created by setting it to zero.

Fact 7: The potential A_z is *constant* over the surface of either conductor at a fixed z. (3.8.11)

Proof A: Consider putting a narrow sensing math loop in Fig. 3.5 perpendicular to the plane of paper. When such a loop is parallel to the B lines, there is no threading B flux. Since B = curlA, this means from (1.1.39) that $\oint_C \mathbf{A} \bullet d\mathbf{s} = 0$ so that that A_z is then constant on both long sides of such a loop. In other words, since B = curlA, the B field lines represent contours of constant A_z.

According to (3.7.8) the B field lines just above the surface of a conductor run parallel to the surface, regardless of the cross sectional shape. These B lines cannot "dip" into the surface. Thus, since B field lines are surfaces of constant A_z, we conclude that A_z must be constant on either conductor surface in a slice at fixed z.

Fact 7 is true regardless of that fact that there can be considerable non-uniformity of the current density J_z inside a conductor, see the Comment below (3.7.8).

Proof B: Since Fact 7 is important, and is non-obvious, we give here another proof. According to (1.5.5), the King gauge condition div**A** = $-j(\beta^2/\omega)\varphi$ relates **A** and φ. We have argued in Fact 4 that, at least in the dielectric region between the conductors, we can neglect all components of **A** except A_z. In this case, the gauge condition reads $\partial_z A_z = -j(\beta^2/\omega)\varphi$. Now, as we will soon be doing in Chapter 4, assume a separation of variables so that

$$A_z(x,y,z) = (\mu/2\pi)\, i(z)\, A_{zt}(x,y) \quad . \tag{3.8.12}$$

This separation is justified in the "transmission line limit" to be discussed in Chapter 4. If we insert this separated form into $\partial_z A_z = -j(\beta^2/\omega)\varphi$, we end up with,

$$\partial_z A_z = (\mu/2\pi)\, \partial_z i(z)\, A_{zt}(x,y) = \partial_z i(z)\, [A_z / i(z)]$$

so

$$[\partial_z i(z) / i(z)]\, A_z(x,y,z) = -j(\beta^2/\omega)\, \varphi(x,y,z) \quad . \tag{3.8.13}$$

Thus, since φ is constant over a cross section conductor surface according to Fact 6, we conclude that A_z must also be constant over the same surface, since there are no other functions of (x,y) in the above equation. This concludes Proof B.

Proof C: Here is one more proof, a variant of Proof A. We know that **B** = curl **A**. We can construct a cylindrical coordinate system in Fig 3.3 based on a center line that matches the curvature of the surface at the point shown. Let the surface point be distance r from the coordinate system axis. In this system we find that

$$B_{\mathbf{r}} = [\text{curl } \mathbf{A}]_{\mathbf{r}} \;=\; (1/r)\partial_{\boldsymbol{\theta}}A_{\mathbf{z}} - \partial_{\mathbf{z}}A_{\boldsymbol{\theta}} \;\approx\; (1/r)\partial_{\boldsymbol{\theta}}A_{\mathbf{z}} \;. \qquad (3.8.14)$$

But, according to (3.7.8) $B_{\mathbf{r}} = 0$. Thus, $\partial_{\boldsymbol{\theta}}A_{\mathbf{z}} = 0$. This says that $A_{\mathbf{z}}$ does not change as one moves along the cross section surface of a conductor, since this is locally always the θ direction. Thus, $A_{\mathbf{z}}$ is constant over the surface at fixed z.